Optimal Placement for Barrier Coverage in Bistatic Radar Sensor Networks

Xiaowen Gong, *Student Member, IEEE*, Junshan Zhang, *Fellow, IEEE*, Douglas Cochran, *Senior Member, IEEE*, and Kai Xing, *Member, IEEE, ACM*

***Abstract*—By taking advantage of active sensing using radio waves, *radar* sensors can offer several advantages over passive sensors. Although much attention has been given to multistatic and multiple-input–multiple-output (MIMO) radar concepts, little has been paid to understanding radar networks (i.e., multiple individual radars working in concert). In this context, we study the coverage problem of a *bistatic radar* (BR) sensor network, which is very challenging due to the *Cassini oval* sensing region of a BR and the coupling of sensing regions across different BRs. In particular, we consider the problem of deploying a network of BRs in a region to maximize the *worst-case intrusion detectability*, which amounts to minimizing the *vulnerability* of a *barrier*. We show that it is optimal to place BRs on the *shortest barrier* if it is the shortest line segment that connects the left and right boundary of the region. Based on this, we study the optimal placement of BRs on a line segment to minimize its vulnerability, which is a nonconvex optimization problem. By exploiting certain specific structural properties pertaining to the problem (particularly an important structure of detectability), we characterize the optimal *placement order* and the optimal *placement spacing* of the BR nodes, both of which present elegant *balanced* structures. Our findings provide valuable insights into the placement of BRs for barrier coverage. To our best knowledge, this is the first work to explore the barrier coverage of a network of BRs.**

***Index Terms*—Barrier coverage, bistatic radar sensor network, optimal placement, worst-case intrusion.**

I. Introduction

WIRELESS sensor networks have received tremendous attention over the past decade. Typically, it is assumed that a sensor network is composed of *passive sensors* (e.g., thermal, acoustics, optic sensors) that detect radiation that is emitted or reflected by an object. In contrast, active RAdio Detection And Ranging (*radar*) purposefully emits radio waves with the objective of collecting echoes. The ability to design the structure and power of the transmitted radio signal imbues active radars with performance advantages over passive sensors in many application scenarios, though this is typically at the expense of additional system complexity.

Thanks to recent technological advances, radars are becoming less expensive and more compact, making it feasible to deploy a network of radars working in concert. Indeed, the application scale and scope of networked radar sensors[1] are expected to expand significantly. Due to the advantages of radars over traditional passive sensors, radar networks have great potential for many applications, such as border security [2] and traffic monitoring [3]. Nevertheless, to fully exploit this potential, radar networks should be judiciously designed.

Coverage, which defines how well the object of interest is monitored, is a critical performance metric for sensor networks. *Barrier coverage* has recently emerged as an efficient coverage strategy for numerous sensor network applications centered around *intruder detection*, such as border monitoring and drug interdiction, and has drawn a surge of research interest [4]–[7]. Despite tremendous research efforts on coverage problems for sensor networks [8], those pertaining to radar sensors remain largely unexplored, and this is the main subject of this paper.

In this paper, we consider the problem of deploying a network of bistatic radars (BRs) for intrusion detection (as illustrated in Fig. 1). Due to the flexibility to deploy the radar transmitter and receiver separately, a BR is more favorable than a monostatic radar (MR) for coverage. Our goal is to *build a fundamental understanding of a bistatic radar network (BRN) for coverage*. In particular, a central question we ask here is the following: *Where should the BRs be placed to achieve the optimal coverage quality?*

The coverage problem of a BRN is dramatically different and more challenging than that of a network of traditional passive sensors because: 1) departing from the disk sensing region of a

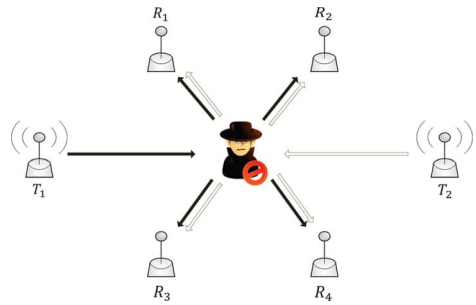

Fig. 1. Example of a bistatic radar network consisting of two radar transmitters T_1, T_2 and four radar receivers R_1, R_2, R_3, R_4. Each transmitter–receiver pair operates as a bistatic radar.

Manuscript received November 02, 2013; revised August 11, 2014; accepted September 13, 2014; approved by IEEE/ACM TRANSACTIONS ON NETWORKING Editor S. Chen. Date of publication October 17, 2014; date of current version February 12, 2016. This work was supported in part by the NSF under Grant CNS-0901451, the U.S. AFOSR under Project FA9550-10-1-0464, the DoD MURI under Project No. FA9550-09-1-0643, and the NSFC under Grant 61170267. A preliminary version of this manuscript has been presented at the ACM International Symposium on Mobile Ad Hoc Networking and Computing (MobiHoc), Bangalore, India, July 29–August 1, 2013.

X. Gong, J. Zhang, and D. Cochran are with the School of Electrical, Computer, and Energy Engineering, Arizona State University, Tempe, AZ 85287 USA (e-mail: xgong9@asu.edu; junshan.zhang@asu.edu; cochran@asu.edu).

K. Xing is with the School of Computer Science and Technology, University of Science and Technology of China, Hefei 230027, China (e-mail: kxing@ustc.edu.cn).

Color versions of one or more of the figures in this paper are available online at http://ieeexplore.ieee.org.

Digital Object Identifier 10.1109/TNET.2014.2360849

[1]For brevity, we use "radar" and "radar sensor" interchangeably.

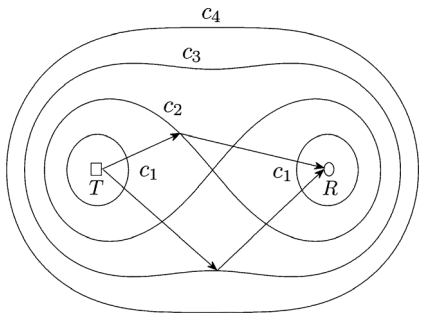

Fig. 2. Bistatic radar SNR contours are Cassini ovals with foci at BR transmitter T and receiver R for different distance products: $c_1 < c_2 < c_3 < c_4$.

passive sensor, the sensing region of a BR depends on the locations of both the transmitter and receiver and is characterized by a Cassini oval. Formally, a Cassini oval is a locus of points for which the distances to two fixed points (foci) have a constant product (as illustrated in Fig. 2); 2) the sensing regions of different BRs are coupled with each other since each BR transmitter[2] (or receiver) can potentially pair with different BR receivers (or transmitters, respectively) to form multiple BRs such that its location would impact multiple BRs.

Next, we summarize the main contributions of this paper.

- We consider the problem of deploying a network of BRs in a region to maximize the *worst-case intrusion detectability*, which is equivalent to minimizing the *vulnerability* of the optimal *barrier* in the region. We show that it is optimal to place BRs on the *shortest barrier* if it is the shortest line segment that connects the left and right boundary of the region.
- The main thrust of this paper is devoted to characterizing the optimal placement of BRs on a line segment to minimize its vulnerability, *which is a highly nontrivial optimization problem due to its nonconvexity*. To tackle the challenges herein, we recast the problem as finding the optimal *placement order* of BR nodes with the optimal *placement spacing*. Based on an important structure of detectability, we characterize *balanced* placement spacing and show that it is optimal. Using the optimal placement spacing, we then characterize the optimal placement orders, which also present balanced structures. These findings provide valuable insights into the placement of BRs for barrier coverage.

Although it is somewhat idealized, the Cassini oval sensing model [see signal-to-noise ratio (SNR) equation (1)] used in this paper can capture the essential feature of a BR, compared to a passive sensor or MR. Furthermore, the coverage problem of a BRN corresponding to the Cassini oval sensing model gives rise to significant technical difficulties (as will be seen later). Needless to say, future work is needed to generalize this study to more complex and realistic situations. In short, we believe that this paper will open a new door to explore radar sensor networks.

The rest of this paper is organized as follows. Section II introduces the model of bistatic radar network and the worst-case coverage and defines the optimal placement problem. In Section III, we address the optimal placement problem based on the barrier coverage strategy. We study the optimal placement of BRs on a line segment in Section IV. Numerical results are provided in Section V, and related work is reviewed in Section VI. Section VII concludes this paper and discusses future work.

II. Model and Problem Definition

In this section, we first describe the model of bistatic radar network and the worst-case coverage, and then define the optimal placement problem.

A. Bistatic Radar Network

The radar transmitter and receiver of a BR are at different locations, whereas they are co-located for an MR. Intuitively, a BR can achieve better coverage than an MR by appropriate placement of the transmitter and receiver, such that the target is more likely to be physically closer to either the transmitter or receiver, and thus attains a high SNR. This advantage of BR will be illustrated by an example in Section III.

One fundamental metric of target detection for a BR is its received SNR: The strength of the received radar signal indicates how likely the target is present. Let $\|AB\|$ and $\overline{AB}$ denote the (Euclidean) distance and the line segment between points A and B, respectively. For convenience, we also use T_i or R_j to denote the location (point) of a transmitter node T_i or receiver node R_j, respectively. For a BR T_i-R_j, the received SNR from the target located at a point X is given by [9]

$$\text{SNR} = \frac{K}{\|T_iX\|^2\|R_jX\|^2} \tag{1}$$

where K denotes a *bistatic radar constant* that reflects physical characteristics of the BR, such as transmit power, *radar cross section*,[3] and antenna power gains. The SNR contours of a BR are characterized by the Cassini ovals with foci at the transmitter and receiver of the BR.

For a network of BRs, we assume that all transmitters operate on orthogonal radio resources (e.g., by using orthogonal waveforms [10]–[13]) to avoid mutual interference at a receiver. While multiple receivers can pair with the same transmitter to form multiple BRs, a receiver can also pair with multiple transmitters. Typically, a BRN has more receivers than transmitters, mainly because that a transmitter incurs higher cost than a receiver (e.g., since signal transmission consumes more energy than other sensor activities such as signal reception and processing). In addition, the number of transmitters can also be limited by the available radio resources (e.g., the number of orthogonal waveforms).

We consider the deployment of a BRN consisting of M transmitters $T_i \in \mathcal{T}$, $i \in \mathcal{M} \triangleq \{1, \ldots, M\}$ and N receivers $R_j \in \mathcal{R}$, $j \in \mathcal{N} \triangleq \{1, \ldots, N\}$. We assume that transmitters and receivers, respectively, have homogeneous physical characteristics such that all BRs have the same bistatic radar constant. We assume that a receiver can potentially pair with all transmitters to form multiple BRs. However, in Section IV, we will show

[2]For brevity, we use "transmitter" and "BR transmitter," "receiver" and "BR receiver" interchangeably, respectively.

[3]Radar cross section measures the amount of radar signal energy reflected by an object depending on its physical characteristics (e.g., shape, material).

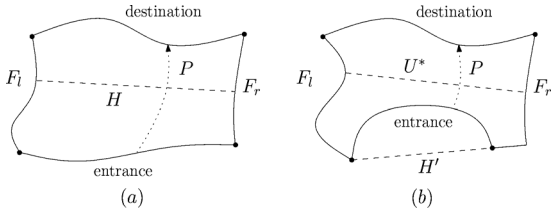

Fig. 3. Examples of the region of interest F. (a) H is the shortcut barrier. (b) H' is the shortest line segment that connects $F_{\rm l}$ and $F_{\rm r}$ but is not a barrier, and thus the shortcut barrier does not exist; the shortest barrier U^* is a line segment but is not the shortcut barrier.

that it suffices for a receiver to pair with *at most two* transmitters. We also assume that transmitters and receivers are *omnidirectional*. We further assume that the radar signals reflected by the target are *omnidirectional*.[4]

B. Worst-Case Coverage

The BRN is deployed in a 2-D geographical *region of interest* F to detect an intruder that traverses through the region. The region F is defined by an entrance side, a destination side, a left boundary $F_{\rm l}$, and a right boundary $F_{\rm r}$ (as illustrated in Fig. 3). The intruder can choose any *intrusion path* P in region F that connects the entrance to the destination.

Existing studies on sensor network coverage [15]–[17] use the distance from a point to its *closest* sensor to measure the coverage of the point (also known as the *closest sensor observability*). In the same spirit, we measure the coverage of a point by the *highest* SNR received by a BR among all BRs, when the target is present at the point. In Section IV-D, we will discuss the case where data fusion is used such that the coverage depends on the SNRs received by multiple BRs. Considering (1), we have the following definition.

Definition 1 (Detectability): The *detectability*[5] of a point X, denoted by $I(X)$, is the minimum distance product of X with respect to a BR among all BRs

$$I(X) \triangleq \min_{T_i\in\mathcal{T},R_j\in\mathcal{R}} \|T_iX\|\|R_jX\|. \tag{2}$$

In other words, the detectability of a point is determined by the *closest* BR to the point, which consists of its closest transmitter and closest receiver. Similar to [15]–[17], we use the *worst-case intrusion* to quantify the coverage of the intruder.

Definition 2 (Worst-Case Intrusion [15]): The *worst-case intrusion path*, denoted by P^*, is the intrusion path with the minimum detectability among all possible intrusion paths

$$P^* \triangleq \arg\max_{P\in\mathcal{P}} D(P) \tag{3}$$

where $\mathcal{P}$ denotes the set of all possible intrusion paths, and $D(P)$ denotes the detectability of intrusion path P, which is the maximum detectability of a point among all the points in P

$$D(P) \triangleq \min_{X\in P} I(X). \tag{4}$$

[4]The reflected radar signals may not be omnidirectional. For the sake of tractability, most of the literature on bistatic radar (e.g., [2], [9], and [14]) assumes that they are omnidirectional.

[5]With a little abuse of notation, we use $I(X)$ to denote the detectability of X, while the detectability of X changes inversely with the value of $I(X)$.

C. Problem Definition

We are interested in finding the optimal placement of the BRN (i.e., the optimal locations of M transmitters and N receivers) in region F that maximizes the worst-case intrusion detectability

$$\underset{T_i\in F,R_j\in F}{\text{minimize}}\ D(P^*). \tag{5}$$

Based on the notion of worst-case coverage, problem (5) is of great interest for the intruder detection problem. In particular, solving (5) provides the answer to an important question: How many transmitters and receivers are needed, and where should they be placed to provide the required coverage quality such that *at least one* BR will receive an SNR above a predefined threshold, regardless of the intruder's path?

Note that problem (5) is difficult to solve in general (even for sensors with disk sensing regions). This is because the shape of region F can be arbitrary, and the feasible solution space contains infinitely many placements in region F.

III. Placement for Barrier Coverage

In this section, we address problem (5) using the approach of barrier coverage. We show that under certain conditions it is optimal to place BRs on the shortest barrier in the region, in which case it is a line segment. We also investigate the placement on the shortest barrier that is an arbitrary curve. All the proofs of this paper are relegated to the Appendix.

A. Optimality Condition for Shortest-Barrier-Based Placement

Similar to [4]–[7], we define a *barrier* as a curve in region F such that *any* intrusion path intersects with the curve. We use the following concept as the coverage metric of a barrier.

Definition 3 (Vulnerability): The vulnerability $V(U)$ of a barrier U is the minimum detectability of a point among all the points in U

$$V(U) \triangleq \max_{X\in U} I(X). \tag{6}$$

The rationale of using vulnerability as the coverage metric is that since a barrier intersects with any possible intrusion path, the vulnerability of a barrier serves as an *upper bound* on the worst-case intrusion detectability. Furthermore, this bound is *tight* when all the barriers are taken into account, such that

$$D(P^*) = \min_{U\in\mathcal{U}} V(U) \tag{7}$$

where $\mathcal{U}$ denotes the set of all the barriers in region F.

Using (7), (5) boils down to finding the *optimal barrier*, which is the optimal solution of the following problem:

$$\underset{U\ \in\ \mathcal{U}}{\text{minimize}}\ V^*(U) \tag{8}$$

where $V^*(U)$ denotes the minimum vulnerability of U, which is the optimal value of the following problem:

$$\underset{T_i\in F,R_j\in F}{\text{minimize}}\ V(U). \tag{9}$$

It is plausible that the optimal barrier for (8) should be the *shortest barrier*, denoted by U^*, which is the barrier with the minimum length among all the barriers. However, this strategy is not optimal in general because $V^*(U^*)$ can be greater than $V^*(U)$ for a barrier U with a greater length than U^*. We give an illustrative example in Fig. 4. For line segment $\overline{AB}$ in Fig. 4(a), it is clear that the optimal placement of a BR T_1-R_1 that minimizes $V(\overline{AB})$ is to set $\|AT_1\| = \|R_1B\| = \sqrt{2}-1$ such that

$V^*(\overline{AB}) = \|AT_1\|\|AR_1\| = 1$. For curve $\widetilde{CF}$[6] in Fig. 4(b), it has a greater length than $\overline{AB}$, while we have $V^*(\widetilde{CF}) \leq V(\widetilde{CF}) = \|TE\|\|ER\| = \sqrt{5}/4 < 1 = V^*(\overline{AB})$, where $V(\widetilde{CF})$ denotes the vulnerability of $\widetilde{CF}$ when T_1 and R_1 are placed at the midpoint of $\overline{CD}$ and $\overline{EF}$, respectively. Therefore, if $\overline{AB}$ is the shortest barrier in region F while $\widetilde{CF}$ is another barrier in F (which is possible), the optimal barrier cannot be $\overline{AB}$.

Before proceeding further, we use a simple example to illustrate the advantage of a BR over an MR for barrier coverage. If we place an MR (which consists of a pair of co-located radar transmitter and receiver) on $\overline{AB}$ in Fig. 4(a) to minimize $V(\overline{AB})$, the optimal placement location is clearly at the midpoint Y_{AB} of $\overline{AB}$ such that $V(\overline{AB}) = \|AY_{AB}\|^2 = 2$. This is greater than $V^*(\overline{AB}) = 1$ which is achieved under the optimal placement of a BR T_1-R_1.

Although it is in general not optimal to place BRs on the shortest barrier U^*, this strategy is optimal if U^* is also the *shortcut barrier* defined as follows.

Definition 4 (Shortcut Barrier): The shortcut barrier, denoted by H, exists and is the shortest barrier U^* if and only if U^* is the shortest line segment that connects left boundary $F_{\rm l}$ and right boundary $F_{\rm r}$ (i.e., the length of U^* is the minimum distance between a point in $F_{\rm l}$ and a point in $F_{\rm r}$).

Although the shortest line segment that connects $F_{\rm l}$ and $F_{\rm r}$ always exists, it may not be in region F, and therefore is not a barrier [as illustrated in Fig. 3(b)]. The shortcut barrier exists for a large class of shapes of region F (e.g., any convex region). Note that if the shortest barrier U^* is also the shortcut barrier, then U^* must be a line segment; otherwise, U^* may or may not be a line segment [as illustrated in Fig. 3(b)]. We next show that the existence of the shortcut barrier is the optimality condition.

Theorem 1: If the shortcut barrier H exists, then H is the optimal barrier for (8). As a result, it suffices to solve (9) for H in order to solve (5).

Note that Theorem 1 provides a *sufficient* condition under which the optimal barrier is the shortest barrier. With regard to the optimal placement of BRs for a line segment, we have the following result.

Proposition 1: For a line segment $\overline{AB}$, the optimal placement for problem (9) for $\overline{AB}$ is on $\overline{AB}$, and the optimal value of (9) for $\overline{AB}$ increases as its length $\|AB\|$ increases.

The proof is based on a similar argument as in the proof of Theorem 1 and is thus omitted. By Theorem 1 and Proposition 1, as it is optimal to place BRs on the shortcut barrier H, which is a line segment. In Section IV, we will focus on finding the optimal placement of BRs on a line segment that minimize its vulnerability.

B. Placement on Curved Shortest Barrier

If the shortest barrier U^* is not the shortcut barrier, it can be an arbitrary curve and may not be the optimal barrier for (8). Furthermore, it is in general difficult to find the optimal placement for (9) for an arbitrary curve (even for sensors with disk sensing regions). In this case, we can find a placement $\{\mathcal{T}', \mathcal{R}'\}$ on U^* that *imitates* the optimal placement $\{\mathcal{T}, \mathcal{R}\}$ for (9) for a line segment $\overline{U^*}$ that has the same length as U^*, such that $\|AT_1\| = \|\widetilde{A'T_1'}\|$, $\|T_1T_2\| = \|\widetilde{T_1'T_2'}\|, \ldots, \|T_MB\| = \|\widetilde{T_M'B'}\|$ and $\|AR_1\| = \|\widetilde{A'R_1'}\|$, $\|R_1R_2\| = \|\widetilde{R_1'R_2'}\|, \ldots, \|R_MB\| = \|\widetilde{R_M'B'}\|$, where A, B are the endpoints of $\overline{U^*}$ and A', B' are the endpoints U^*. We use an example in Fig. 4(a) and (c) to illustrate the imitation placement. It has an appealing property as stated in the following result.

[6]We use $\widetilde{PQ}$ to denote a curve with endpoints P, Q, and $\|\widetilde{PQ}\|$ to denote its length.

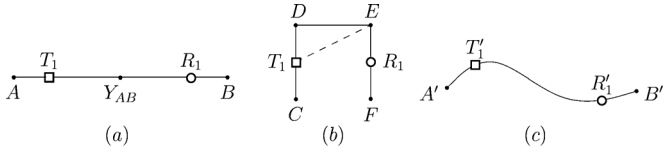

Fig. 4. Example where $\|AB\| < \|\widetilde{CF}\|$ but $V^*(\overline{AB}) > V^*(\widetilde{CF})$ under the placement of a BR T_1-R_1. (a) $\|AB\| = 2\sqrt{2}$, $\|AT_1\| = \|R_1B\| = \sqrt{2} - 1$. (b) $\|CD\| = \|DE\| = \|EF\| = 1$, $\overline{CD} \perp \overline{DE}$, $\overline{EF} \perp \overline{DE}$, $\|CT_1\| = \|R_1F\| = 1/2$. The placement $\{T_1', R_1'\}$ on $\widetilde{A'B'}$ imitates the placement $\{T_1, R_1\}$ on $\overline{AB}$ where $\|AB\| = \|\widetilde{A'B'}\|$. (c) $\|\widetilde{A'B'}\| = 2\sqrt{2}$, $\|\widetilde{A'T_1'}\| = \|\widetilde{R_1'B'}\| = \sqrt{2} - 1$.

TABLE I
FREQUENTLY USED NOTATIONS

Notation	Description
$\overline{AB}$	line segment between point A and B
$\|AB\|$	distance between point A and B (length of $\overline{AB}$)
Y_{AB}	midpoint of $\overline{AB}$
M, N	total number of BR transmitters, BR receivers
$\mathcal{T}$, $\mathcal{R}$	set of all BR transmitters, BR receivers
T_i, R_j	BR transmitter i, BR receiver j
T_i-R_j	BR consisting of T_i and R_j
$I(X)$	detectability of X
$V(\overline{AB})$	vulnerability of $\overline{AB}$
H, h	shortcut barrier and its length
H_l, H_r	left and right endpoint (node) of H
$\mathcal{S}$	placement of $\mathcal{T}$, $\mathcal{R}$, H_l, and H_r on a line
$\mathbf{S}$, $\mathbf{D_S}$	placement order and its placement spacing
$\mathbf{S}_i$, $\mathbf{D}_{\mathbf{S}_i}$	independent local placement order and its local placement spacing
$Z_{\mathbf{S}_i}$, $L_{\mathbf{S}_i}$	local zone of $\mathbf{S}_i$ and its length
e_c^i	parameter that characterizes balanced spacing

Proposition 2: For the optimal placement $\{\mathcal{T}, \mathcal{R}\}$ on the line segment $\overline{U^*}$ and the imitation placement $\{\mathcal{T}', \mathcal{R}'\}$ on the shortest barrier U^*, we have $V^*(\overline{U^*}) \geq V'(U^*)$.

The proof is based on a similar argument as in the proof of Theorem 1 and is thus omitted. By Proposition 2, $V^*(\overline{U^*})$ is no less than $V(U^*)$ under the imitation placement, and thus $V^*(\overline{U^*})$ serves as an upper bound for the worst-case intrusion detectability $D(P^*)$, which is the objective that we aim to minimize [i.e., the objective value of problem (5)]. Since the shortest barrier U^* has the minimum length among all the barriers, according to Proposition 1, the imitation placement on U^* gives the *minimum* upper bound $V^*(\overline{U^*})$ for $D(P^*)$ among all the barriers.

IV. OPTIMAL PLACEMENT ON A LINE SEGMENT

In this section, we study the optimal placement of BRs on a line segment, say the shortcut barrier H, to minimize its vulnerability $V(H)$.

A. Problem Recast

Let $H_{\rm l}$ and $H_{\rm r}$ be the left and right endpoint of H, respectively, and h be the length of H. For convenience, we list the frequently used notations in Table I. Also let $t_i \triangleq \|H_{\rm l}T_i\|$ and $r_j \triangleq \|H_{\rm l}R_j\|$. Mathematically, our problem can be written as

$$\begin{aligned} \underset{t_i,r_j}{\text{minimize}} \quad & \max_{0\le x\le h} \min_{i\in\mathcal{M},j\in\mathcal{N}} |x-t_i||x-r_j| \\ \text{subject to} \quad & 0\le t_i\le h \qquad \forall i\in\mathcal{M} \\ & 0\le r_j\le h \qquad \forall j\in\mathcal{N} \end{aligned} \tag{10}$$

where $\min_{i\in\mathcal{M},j\in\mathcal{N}}|x-t_i||x-r_j|$ represents the detectability of a point $X \in H$ with $\|H_{\rm l}X\| = x$, and $\max_{0\le x\le h}\min_{i\in\mathcal{M},j\in\mathcal{N}}|x-t_i||x-r_j|$ represents the vulnerability of H. In general, we can show that (10) is *nonconvex*. Therefore, standard optimization methods would not work well here.

To gain useful insight into (10), we view the line-segment-based placement in an intuitive way as follows. First, we treat $H_{\rm l}$ and $H_{\rm r}$ as two (virtual) nodes and relax the constraint $\|H_{\rm l}H_{\rm r}\| = h$. Then, we place all the BR nodes $\mathcal{T}$ and $\mathcal{R}$ as well as $H_{\rm l}$ and $H_{\rm r}$ on a horizontal line subject to the constraint that $H_{\rm l}$ and $H_{\rm r}$ are the *leftmost* and *rightmost* nodes, respectively. We can use the following concepts to characterize any placement on a line.

Definition 5 (Placement Order and Spacing): A *placement order* (referred to as "order" for brevity) $\mathbf{S}$ is an order of all the nodes on the line from left to right

$$\mathbf{S} \triangleq (H_{\rm l}, S_1, \ldots, S_J, H_{\rm r})$$

where $J \triangleq M+N$ and $(S_1,\ldots,S_J)$ is a permutation of the BR nodes such that $\|H_{\rm l}H_{\rm l}\| \le \|H_{\rm l}S_1\| \le \ldots \le \|H_{\rm l}S_J\| \le \|H_{\rm l}H_{\rm r}\|$. The *placement spacing* (referred to as "spacing" for brevity) $\mathbf{D_S}$ of a placement order $\mathbf{S}$ consists of the distances each between a pair of neighbor nodes in $\mathbf{S}$

$$\mathbf{D_S} \triangleq (\|H_{\rm l}S_1\|, \ldots, \|S_JH_{\rm r}\|).$$

A *local placement order* (referred to as "local order" for brevity) $(S_{i+1},\ldots,S_{i+j})$ is an order of a set of neighbor nodes in $\mathbf{S}$, and its placement spacing is

$$\mathbf{D}_{(S_{i+1}\ldots,S_{i+j})} \triangleq (\|S_{i+1}S_{i+2}\|, \ldots, \|S_{i+j-1}S_{i+j}\|).$$

We can see that any order $\mathbf{S}$ with any spacing $\mathbf{D_S}$ characterize a unique placement of BRs on a line segment with length $\|H_{\rm l}H_{\rm r}\|$; conversely, any placement of BRs on the line segment H can be uniquely characterized by some order $\mathbf{S}$ with some spacing $\mathbf{D_S}$ that satisfies $\|H_{\rm l}H_{\rm r}\| = h$. Therefore, our problem (10) can be recast as

$$\begin{aligned} \underset{\mathbf{S},\mathbf{D_S}}{\text{minimize}} \quad & V(\overline{H_{\rm l}H_{\rm r}}) \\ \text{subject to} \quad & \|H_{\rm l}H_{\rm r}\| = h. \end{aligned} \tag{11}$$

It is clear that the optimal value of (11) increases as h increases. As a result, we can formulate a problem relevant to (11) as \

$$\begin{aligned} \underset{\mathbf{S},\mathbf{D_S}}{\text{maximize}} \quad & \|H_{\rm l}H_{\rm r}\| \\ \text{subject to} \quad & V(\overline{H_{\rm l}H_{\rm r}}) \le c. \end{aligned} \tag{12}$$

Let l_c denote the optimal value of (12) under the constraint $V(\overline{H_{\rm l}H_{\rm r}}) \le c$. It is also clear that l_c is increasing in c and, in particular, $l_c \to 0$ when $c \to 0$ and $l_c \to \infty$ when $c \to \infty$. Therefore, if we can solve (12) for any $c > 0$, we can also solve (11) by a *bisection search* as described in Algorithm 1.

Algorithm 1: Compute the optimal placement for problem (11)

input : line segment length h, precision threshold ϵ
output: optimal order $\mathbf{S}^*$, optimal spacing $\mathbf{D}^*_{\mathbf{S}^*}$, optimal value c^*

$c_1 \leftarrow 0$, $c_2 \leftarrow h^2$, $c \leftarrow \frac{c_1+c_2}{2}$;
repeat
  Compute the optimal order $\mathbf{S}^*$ and the optimal spacing $\mathbf{D}^*_{\mathbf{S}^*}$ for problem (12) subject to $V(\overline{H_lH_r}) \le c$;
  if $l_c > h+\epsilon$ **then**
    $c_2 \leftarrow c$; $c \leftarrow \frac{c_1+c_2}{2}$;
  end
  if $l_c < h-\epsilon$ **then**
    $c_1 \leftarrow c$; $c \leftarrow \frac{c_1+c_2}{2}$;
  end
until $|c-c_1| \le \epsilon$;
return $\mathbf{S}^*$, $\mathbf{D}^*_{\mathbf{S}^*}$, $c^* \leftarrow c$;

Specifically, Algorithm 1 keeps track of an interval $[c_1, c_2]$ that must contain the optimal value c^* of (11), and reduce the interval by half at each step, until the interval is sufficiently small such that the difference between c^* and the endpoint c_1 or c_2 is upper-bounded by a predefined precision threshold ϵ. Since the initial interval is set to $[0, h^2]$, the number of steps for running Algorithm 1 is upper-bounded by $O(\log(h^2/\epsilon))$.

We make two observations regarding any placement of BRs. First, since all BRs are homogeneous, *swapping* the locations of any pair of transmitters (or receivers, respectively) results in an equivalent placement. Second, transmitters and receivers are *reciprocal* in the sense that replacing all transmitters by receivers while replacing all receivers by transmitters results in an equivalent placement. As a result, for ease of exposition, in the rest of this paper we assume that $M \le N$. All the analysis hereafter can directly apply to the case $M > N$ by treating transmitters as receivers while treating receivers as transmitters.

B. Optimal Placement Order and Spacing

In this section, our goal is to characterize the optimal order and the optimal spacing for problem (12). We outline the major steps to achieve this goal as follows.

1) We show an important structure of detectability for any placement on a line (Lemma 1), based on which we define *balanced spacings* and *independent local orders*.
2) We characterize the balanced local spacing for an independent local order (Lemma 2) and show that it is optimal (Lemma 3).
3) We show that the balanced spacing for a *dividable* order consists of balanced local spacings for independent local orders, and it is optimal (Theorem 2).
4) We show that there exist optimal orders in the class of dividable orders (Lemma 4), based on which we characterize the optimal orders (Theorem 3).

We start with the observation that the optimal order $\mathbf{S}^*$ for (12) is equivalent to the optimal order of the following problem:

$$\underset{\mathbf{S}}{\text{maximize}} \ f_c^{\mathbf{S}} \tag{13}$$

where $f_c^{\mathbf{S}}$ denotes the optimal value of the following problem for order $\mathbf{S}$:

$$\begin{aligned} \underset{\mathbf{D_S}}{\text{maximize}} \quad & \|H_{\rm l}H_{\rm r}\| \\ \text{subject to} \quad & V(\overline{H_{\rm l}H_{\rm r}}) \le c. \end{aligned} \tag{14}$$

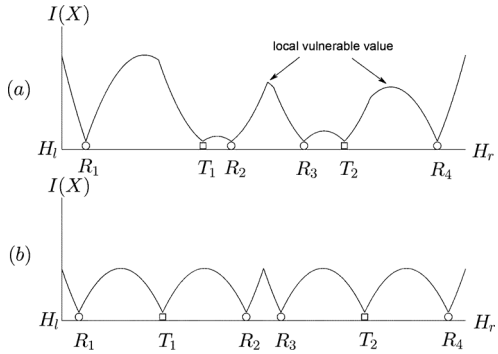

Fig. 5. Local vulnerable values are (a) unequal under arbitrary placement spacing and (b) equal under balanced placement spacing.

Therefore, the optimal spacing $\mathbf{D}^*_{\mathbf{S}^*}$ for (12) is equivalent to the optimal spacing for (14) for the optimal order $\mathbf{S}^*$.

The following lemma presents an important structure of detectability for any placement on a line. We use Y_{AB} to denote the midpoint of a line segment $\overline{AB}$.

Lemma 1: For any order $\mathbf{S}$ with any spacing $\mathbf{D_S}$, the detectability on $\overline{H_\mathrm{l}H_\mathrm{r}}$ attains local maximums at the end nodes and at the midpoint of each pair of neighbor BR nodes (as illustrated in Fig. 5)

$$\arg\max_{X\in\overline{H_\mathrm{l}S_1}} I(X) = H_\mathrm{l} \quad \arg\max_{X\in\overline{S_JH_\mathrm{r}}} I(X) = H_\mathrm{r}$$
$$\arg\max_{X\in\overline{S_iS_{i+1}}} I(X) = Y_{S_iS_{i+1}} \qquad \forall i\in\{1,\ldots,J-1\}.$$

Definition 6 (Local Vulnerable Point): A *local vulnerable point* is a local maximum point of detectability on $\overline{H_\mathrm{l}H_\mathrm{r}}$, and a *local vulnerable value* is its detectability.

By Lemma 1, it suffices to examine the local vulnerable values to determine the vulnerability of a line segment. Based on Lemma 1, we define the following concept.

Definition 7 (Independent Local Order): A local order $\mathbf{S}_i$ is an *independent local order* if it has any of the following *types*:

$$(T,R),(R,T)$$
$$(T,R^k,H_\mathrm{r}),(R,T^k,H_\mathrm{r}),(H_\mathrm{l},R^k,T),(H_\mathrm{l},T^k,R),k\geq 1$$
$$(T,R^k,T),(R,T^k,R),k\geq 1$$

where T^k and R^k denote k consecutive transmitters and receivers, respectively. The *independent local zone* $Z_{\mathbf{S}_i}$ of an independent local order $\mathbf{S}_i$ is the line segment between the two end nodes in $\mathbf{S}_i$, with its length denoted by $L_{\mathbf{S}_i}$.

For any local placement with any independent local order $\mathbf{S}_i$, the *closest* BR for any local vulnerable point on the independent local zone $Z_{\mathbf{S}_i}$ consists of the nodes in $\mathbf{S}_i$. For example, for $\mathbf{S}_i = (T_1,R_1)$, the closest BR for $Y_{T_1R_1}$ is T_1-R_1; for $\mathbf{S}_i=(T_1,R_1,\ldots,R_k,H_\mathrm{r})$, the closest BR for any of $Y_{T_1R_1},\ldots,Y_{R_{k-1}R_k}$, and H_r, consists of transmitter T_1 and some receiver among $R_1,\ldots,R_k$. Therefore, *all the local vulnerable values on* $Z_{\mathbf{S}_i}$, *and hence the vulnerability* $V(Z_{\mathbf{S}_i})$, *are determined by the spacing* $\mathbf{D}_{\mathbf{S}_i}$ *(i.e., independent of any distance not in* $\mathbf{D}_{\mathbf{S}_i}$*)*. Based on this property, the following concept is well defined for an independent local order.

Definition 8 (Balanced Spacing): The spacing $\mathbf{D_S}$ (or local spacing $\mathbf{D}_{\mathbf{S}_i}$) of an order $\mathbf{S}$ (or an independent local order $\mathbf{S}_i$, respectively) is *balanced* if all the local vulnerable values on $\overline{H_\mathrm{l}H_\mathrm{r}}$ (or the independent local zone $Z_{\mathbf{S}_i}$, respectively) are equal (as illustrated in Fig. 5).

The next lemma characterizes the balanced local spacing for an independent local order.

TABLE II
VALUES OF BALANCED SPACING

c	e_c^0	e_c^1	e_c^2	e_c^3	e_c^4
1	2.0000	0.8284	0.6357	0.5359	0.4721
5	4.4721	1.8524	1.4214	1.1983	1.0557
10	6.3246	2.6197	2.0102	1.6947	1.4930
20	8.9443	3.7048	2.8428	2.3966	2.1115

Lemma 2: For any $c>0$, define $e_c^0 \triangleq 2\sqrt{c}$ and let e_c^j denote the unique positive value of x such that

$$\left(\sum_{i=0}^{j-1} e_c^i + \frac{x}{2}\right)\frac{x}{2} = c \tag{15}$$

for each $j\in\mathbb{N}^+$. For any $c>0$ and any independent local order $\mathbf{S}_i$, there exists a unique balanced local spacing $\mathbf{D}_{\mathbf{S}_i}$ such that $V(Z_{\mathbf{S}_i})=c$, and furthermore, it can be characterized by e_c^i, $i\in\mathbb{N}$ as follows: For $\mathbf{S}_i$ with type (T,R) or (R,T)

$$\mathbf{D}_{\mathbf{S}_i} = \left(e_c^0\right);$$

for $\mathbf{S}_i$ with type (T,R^k,H_r) or (R,T^k,H_r)

$$\mathbf{D}_{\mathbf{S}_i} = \left(e_c^0, e_c^1, \ldots, e_c^{k-1}, \frac{e_c^k}{2}\right);$$

for $\mathbf{S}_i$ with type (H_l,R^k,T) or (H_l,T^k,R)

$$\mathbf{D}_{\mathbf{S}_i} = \left(\frac{e_c^k}{2}, e_c^{k-1}, \ldots, e_c^1, e_c^0\right);$$

for $\mathbf{S}_i$ with type (T,R^k,T) or (R,T^k,R), if k is even

$$\mathbf{D}_{\mathbf{S}_i} = \left(e_c^0, e_c^1, \ldots, e_c^{\frac{k}{2}-1}, e_c^{\frac{k}{2}}, e_c^{\frac{k}{2}-1}, \ldots, e_c^1, e_c^0\right);$$

if k is odd

$$\mathbf{D}_{\mathbf{S}_i} = \left(e_c^0, e_c^1, \ldots, e_c^{\frac{k-1}{2}}, e_c^{\frac{k-1}{2}}, \ldots, e_c^1, e_c^0\right).$$

By definition, given c, the value of e_c^i, $i\in\mathbb{N}^+$ can be found iteratively using (15), which decreases as i increases (as shown in Table II).

Based on the independent property, we can cast a problem in the same spirit as (14) but for an independent local order $\mathbf{S}_i$ as

$$\begin{aligned}\underset{\mathbf{D}_{\mathbf{S}_i}}{\text{maximize}} \quad & L_{\mathbf{S}_i}\\ \text{subject to} \quad & V(Z_{\mathbf{S}_i})\leq c.\end{aligned} \tag{16}$$

The next lemma shows that the balanced local spacing is optimal for (16).

Lemma 3: For any $c>0$ and any independent local order $\mathbf{S}_i$, the balanced local spacing $\mathbf{D}_{\mathbf{S}_i}$ such that $V(Z_{\mathbf{S}_i})=c$ is the optimal local spacing for (16).

The next definition presents a useful structure of a class of orders.

Definition 9 (Dividable Order): An order $\mathbf{S}$ is *dividable* if it can be decomposed into independent local orders $\mathbf{S}_1,\ldots,\mathbf{S}_m$ such that: 1) each node in $\mathbf{S}$ is included in some $\mathbf{S}_i$; 2) the last node of $\mathbf{S}_i$ is the first node of $\mathbf{S}_{i+1}$ for each $i=1,\ldots,m-1$. Therefore, the spacing $\mathbf{D_S}$ consists of *disjoint* independent local spacings $\mathbf{D}_{\mathbf{S}_1},\ldots,\mathbf{D}_{\mathbf{S}_m}$. For example, the following order is dividable:

$$\mathbf{S} = (\overbrace{H_\mathrm{l},R_1,R_2,T_1}^{\mathbf{S}_1},\underbrace{R_3,R_4,R_5,T_2}_{\mathbf{S}_2},\overbrace{R_6}^{\mathbf{S}_3},\underbrace{T_3,T_4,H_\mathrm{r}}_{\mathbf{S}_4}). \tag{17}$$

For any placement with any dividable order $\mathbf{S}$, the local vulnerable points on $\overline{H_\mathrm{l}H_\mathrm{r}}$ consists of *disjoint* sets of local vul-

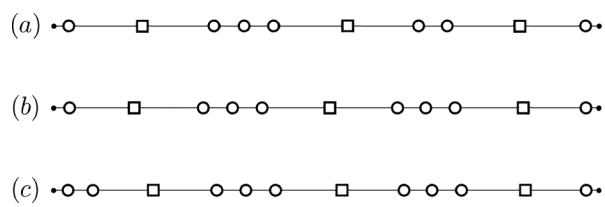

Fig. 6. Optimal placement of transmitters (squares) and receivers (circles) for (a) $M = 3$, $N = 7$; (b) $M = 3$, $N = 8$; (c) $M = 3$, $N = 9$.

nerable points on the independent local zones $Z_{\mathbf{S}_1}, \ldots, Z_{\mathbf{S}_m}$. Therefore, *problem* (16) *for* $\mathbf{S}$ *can be decomposed into independent subproblems, each of which is an instance of problem* (16) *for* $\mathbf{S}_1, \ldots, \mathbf{S}_m$, with the optimal local spacing given by Lemma 3. The next theorem follows from the above observation.

Theorem 2: For any $c > 0$ and any dividable order $\mathbf{S}$, where $\mathbf{S}$ can be decomposed into independent local orders $\mathbf{S}_1, \ldots, \mathbf{S}_m$, the balanced spacing $\mathbf{D}_{\mathbf{S}}$ such that $V(\overline{H_1 H_r}) = c$ exists and consists of the balanced local spacings $\mathbf{D}_{\mathbf{S}_1}, \ldots, \mathbf{D}_{\mathbf{S}_m}$. Furthermore, it is the optimal spacing for (14) for $\mathbf{S}$.

Next, we show that there exist optimal orders in the class of dividable orders. Since all transmitters are homogeneous, we index the transmitters from left to right such that $0 \le \|H_1 T_1\| \le \cdots \le \|H_1 T_M\| \le \|H_1 H_r\|$. Define

$$\mathbf{N}_{\mathbf{S}} \triangleq (n_1, n_2, \ldots, n_M, n_{M+1})$$

where n_i, n_1, n_{M+1} denote the number of receivers in $\mathbf{S}$ between T_{i-1} and T_i for $i \in \{2, \ldots, M\}$, between H_1 and T_1, between T_M and H_r, respectively. Since all transmitters and all receivers are homogeneous, respectively, any order $\mathbf{S}$ can be uniquely characterized by $\mathbf{N}_{\mathbf{S}}$.

Lemma 4: There exists an optimal order $\mathbf{S}^*$ that satisfies the following conditions:

$$\nexists i, j \in \{1, \ldots, M\} \text{ such that } n_i \ge 2,\ n_j = 0 \quad (18a)$$

$$n_2 \ne 0,\ n_M \ne 0. \quad (18b)$$

Furthermore, any order $\mathbf{S}$ that satisfies the above conditions is dividable.

We should note that a nonoptimal order [e.g., the order in (17)] can also be dividable.

Based on Lemma 4, the following theorem provides a *sufficient* condition for the optimal order.

Theorem 3: An order $\mathbf{S}$ is optimal if it satisfies the following conditions:

$$|n_i - n_j| \le 1 \qquad \forall i, j \in \{2, \ldots, M\} \quad (19a)$$

$$|n_i - 2n_1| \le 1, |n_i - 2n_{M+1}| \le 1 \qquad \forall i \in \{2, \ldots, M\}. \quad (19b)$$

Using Theorem 3, we characterize the optimal order $\mathbf{S}^*$ as follows. Let two integers q and r be the quotient and remainder of $\frac{N}{M}$, respectively. If q is even [e.g., as in Fig. 6(a) and (b)], we have

$$\mathbf{N}_{\mathbf{S}^*} = \left(\frac{q}{2}, \overbrace{q+1, \ldots, q+1}^{r}, \overbrace{q, \ldots, q}^{M-1-r}, \frac{q}{2} \right);$$

if q is odd and $r = 0$ [e.g., as in Fig. 6(c)], we have

$$\mathbf{N}_{\mathbf{S}^*} = \left(\frac{q+1}{2}, \overbrace{q, \ldots, q}^{M-1}, \frac{q-1}{2} \right);$$

if q is odd and $r \ge 1$, we have

$$\mathbf{N}_{\mathbf{S}^*} = \left(\frac{q+1}{2}, \overbrace{q+1, \ldots, q+1}^{r-1}, \overbrace{q, \ldots, q}^{M-r}, \frac{q+1}{2} \right).$$

In addition, for any $\mathbf{N}_{\mathbf{S}^*}$, if we swap the values of n_1 and n_{M+1}, or the values of n_i and n_j for $i, j \in \{2, \ldots, M\}$, it also satisfies (19a) and (19b), and hence is optimal.

Given the above optimal order $\mathbf{S}^*$ for (13), which is dividable, we can characterize the optimal spacing $\mathbf{D}^*_{\mathbf{S}^*}$ for (14) using Theorem 2.

C. Remarks

Regarding the analysis and results in Section IV-B, we have the following remarks.

Remark 1: The detectability structure given in Lemma 1 plays a fundamental role in our analysis, based on which the concepts of local vulnerable point, independent local order, balanced spacing, and dividable order can be defined thereafter. This structure is mainly due to that: 1) all BRs are homogeneous; and 2) for any BR, say T_1-R_1, the received SNR from a point on the line segment $\overline{T_1 R_1}$ achieves local minimum at the midpoint $Y_{T_1 R_1}$.

Remark 2: The optimal spacings are *balanced* in the sense that all the local vulnerable values are *equal* under the balanced spacing. The optimality of this balanced structure is due to that minimizing the vulnerability is equivalent to minimizing the maximum local vulnerable value.

The balanced spacing is in general *nonuniform* in the sense that the distance between each pair of neighbor BR nodes is not the same. For the balanced spacing of an independent local order $\mathbf{S}_i$ with type (T, R^k, T), (H_1, R^k, T), or (T, R^k, H_r), the distance between two neighbor receivers decreases as the distance to their closest transmitter increases (i.e., e_c^i decreases as i increases). This nonuniform structure is essentially due to that the detectability of a point is *jointly* determined by its closest transmitter and closest receiver, while the number of transmitters is *unbalanced* with that of receivers.

Remark 3: The optimal orders are also *balanced*, but in a more subtle sense: For the optimal order that satisfies (19), n_i for $i = 2, \ldots, M$ are *as equal as possible*, while each n_i is *as equal as possible to two times* n_1 and n_{M+1}, respectively (as illustrated in Fig. 6). The optimality of this balanced structure is mainly because that the optimal value of (16) for an independent local order $\mathbf{S}_i$ with type (T, R^k, T), (H_1, R^k, T), or (T, R^k, H_r) increases as k increases, while the *marginal increment* decreases as k increases. Therefore, to maximize the sum of the optimal values of (16) for independent local orders $(H_1, \ldots, T_1)$, $(T_1, \ldots, T_2), \ldots, (T_{M-1}, \ldots, T_M)$, $(T_M, \ldots, H_r)$, the optimal order must have that balanced structure.

Remark 4: We can gain useful insights by comparing the placement of BRs on a line segment to that of sensors with disk sensing regions (we assume that they are homogeneous and refer them as "disk sensors" for brevity). For disk sensors, we define the detectability of a point as the distance to its closest sensor. Interestingly, for any placement of disk sensors on a line segment, we can observe the *same* structure as in Lemma 1: The detectability on the line segment also achieves local maximums at the midpoint of each pair of neighbor disk sensors and the

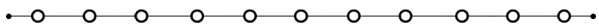

Fig. 7. Optimal placement of disk sensors (circles) has uniform spacing.

endpoints. While this detectability structure is clear for disk sensors (which are homogeneous), it is not obvious for BRs.

Based on the detectability structure, we can show that the balanced spacing is also optimal for disk sensors. However, as illustrated in Fig. 7, the balanced spacing for disk sensors is *uniform* (i.e., each pair of neighbor disk sensors have the same distance), in contrast to that it is nonuniform in general for BRs. We should also note that while the balanced spacing is an *equivalent* condition for the optimal placement of disk sensors, it is only a *necessary* condition for the optimal placement of BRs. This is because different orders of BR nodes can be nonequivalent.

Remark 5: The optimal placement results imply that one assumption made in Section II can be relaxed without losing the optimality. Since the detectability of a point is determined by its closest BR, it suffices for a receiver to pair with a transmitter only if they form the closest BR for some point on the line segment. Therefore, for the optimal placement of a BRN consisting of more receivers than transmitters (e.g., as in Fig. 6), we can see that a receiver only needs to pair with its *closest* transmitter(s), the number of which is *one or two*.

D. Discussions

In this paper, we assume that there is no data fusion among different BRs for target detection. If data fusion is used, the metric of target detection would depend on the SNRs received by multiple BRs (e.g., the sum of the k highest SNRs where $k > 1$) rather than only the highest SNR. As a result, the detectability of a point would depend on its distant product with respect to multiple BRs rather than only the closest BR. As expected, it is very difficult to find the optimal placement of BRs for problem (10) in this case. However, with data fusion, we can show that all the results in Section III (including Theorem 1 and Propositions 1 and 2) still hold via similar analysis, as long as the data fusion model satisfies that target detection improves as the SNR of any BR involved in the data fusion increases (which is typically true). In addition, for the optimal placement on a line segment H under the model without data fusion, we can analyze the coverage quality of this placement under a data fusion model. Specifically, using the detectability of a point as a function of its distances to certain BR nodes (which depends on the data fusion model), we can find the local maximums of the detectability on H (as we do in Lemma 1), and thus the vulnerability of H. Clearly, the vulnerability of H without data fusion serves as an upper bound for that with data fusion.

V. Numerical Results

In this section, we provide numerical results to illustrate the advantage of the optimal placement of BRs on a line segment H.

A. Comparison to Heuristic Placement

As no existing work has studied the placement of BRs for barrier coverage, we compare the optimal placement strategy (OPT) with two heuristic strategies. The heuristics are motivated by the rationale of the optimal placement strategy for a network of homogeneous disk sensors, which is to minimize the maximum distance from a point to its closest sensor among all the points on H.

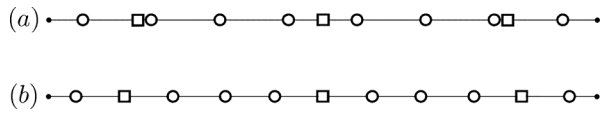

Fig. 8. Heuristic placement of transmitters (squares) and receivers (circles) for $M = 3$, $N = 8$: (a) HEU-1; (b) HEU-2.

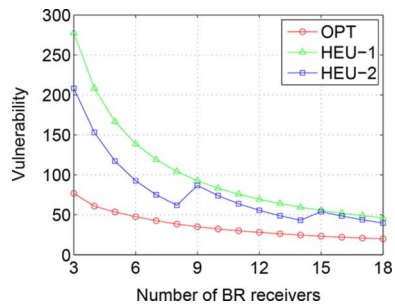

Fig. 9. Vulnerability for three BR transmitters.

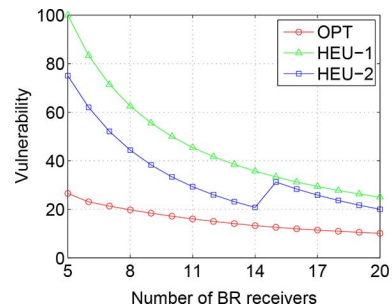

Fig. 10. Vulnerability for five BR transmitters.

The first heuristic (HEU-1) is to place transmitters (or receivers, respectively) with uniform spacing such that the maximum distance from a point on H to its closest transmitter (or receiver, respectively) is minimized [as illustrated in Fig. 8(a)]:

$$2\|H_1T_1\| = \|T_1T_2\| = \cdots = \|T_{M-1}T_M\| = 2\|T_MH_{\mathrm{r}}\|$$
$$2\|H_1R_1\| = \|R_1R_2\| = \cdots = \|R_{N-1}R_N\| = 2\|R_NH_{\mathrm{r}}\|.$$

Comparing Fig. 6(b) to Fig. 8(a) (under the same setting of $M = 3$ and $N = 8$), we can see that neither the placement of transmitters nor receivers in OPT is the same as that in HEU-1. Compared to OPT, the main drawback of HEU-1 is that it places transmitters and receivers *independently*.

The second heuristic (HEU-2) is to place transmitters and receivers according to the optimal order $\mathbf{S}^*$, but with uniform spacing such that the maximum distance from a point on H to its closest BR node (either transmitter or receiver) is minimized [as illustrated in Fig. 8(b)]

$$2\|H_1S_1\| = \|S_1S_2\| = \cdots = \|S_{M-1}S_M\| = 2\|S_MH_{\mathrm{r}}\|.$$

Although HEU-2 follows the optimal order, its main drawback is that it treats transmitters and receivers *equivalently*.

Figs. 9–11 depict the vulnerability of H under OPT, HEU-1, and HEU-2 for a varying number of receivers and three, five, and 10 transmitters, respectively. We set the length of H to 100 m. We observe that HEU-2 results in considerably lower vulnerability than HEU-1, and OPT further outperforms HEU-2 significantly. This shows that OPT is highly advantageous for improving the barrier coverage, which is essentially due to that the design rationale for a BRN under the Cassini oval sensing

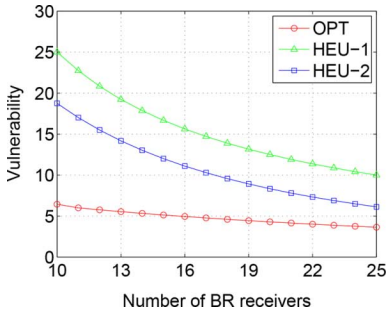

Fig. 11. Vulnerability for 10 BR transmitters.

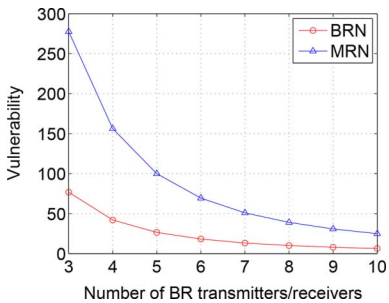

Fig. 12. Minimum vulnerability: BRN versus MRN.

model is quite different from that for a network of passive sensors or MRs under the disk sensing model. Therefore, the optimal placement of a BRN requires judicious design of transmitters and receivers as we do in this paper.

B. Comparison to Monostatic Radar Network

In Fig. 12, we compare the vulnerability of H under the optimal placement of a BRN to that of a monostatic radar network (MRN) for a varying number of transmitters and receivers. The optimal placement strategy for an MRN is to minimize the maximum distance from a point on H to its closest MR. For fair comparison, we set the number of transmitters in the BRN equal to that of receivers, and also equal to the number of MRs in the MRN. We observe that the advantage of a BRN is significant, which demonstrates that the flexibility to place transmitters and receivers separately is highly beneficial for barrier coverage.

VI. Related Work

Radar has been extensively studied for decades [18]. However, radar sensor networks have garnered attention only in the past few years, largely driven by the emergence of cheaper and more compact radar sensors in place of conventionally expensive and bulky radar systems. For example, in [19], a platform has been successfully designed and built to integrate ultrawideband radars with mote-class sensor devices. The existing literature has studied different problems for radar sensor networks, including waveform design and diversity [20], radar scheduling [21], and data management [22] for a variety of objectives, such as target detection [23] and localization [14]. In particular, BRs have also been considered in [14]. However, coverage problems of a radar sensor network have received very little attention. Recently, a novel Doppler coverage model has been introduced in [24] for a radar sensor network that exploits the Doppler effect. To our best knowledge, this work is the first to explore the barrier coverage of a network of BRs.

Numerous studies on sensor network coverage can be found in the literature [8]. Worst-case intrusion was first introduced in [15]. References [15], [16], and [25] have studied how to find the worst-case intrusion path for arbitrarily deployed sensors. References [26] and [27] have considered adding sensors to improve the coverage of the worst-case intrusion path. Along another avenue, barrier coverage was first introduced in [4] and has attracted much research interests recently. References [4] and [6] have studied the critical sensor density for barrier coverage under random deployment. The coverage of a barrier has been investigated using a quantitative metric in [5]. Barrier coverage of sensors with mobility has been considered in [7] and [28]. Barrier coverage for camera sensor networks has also been studied recently based on a novel full-view coverage model [29], [30].

While most aforementioned studies are concerned with how to find the worst-case intrusion path or a barrier covered by sensors (if such a barrier exists) under an *existing* deployment of sensors, our work focuses on *where* to deploy sensors to cover a barrier such that the worst-case intrusion detectability is maximized. More importantly, the existing sensing models (particularly the widely used disk sensing model) are quite different from the Cassini oval sensing model of a BR, and the latter is further complicated by the coupling of sensing regions across multiple BRs.

VII. Conclusion and Future Work

Radar sensor networks have great potential in many applications, such as border surveillance and traffic monitoring. In this paper, we studied the problem of deploying a network of BRs in a region for intruder detection. The optimal placement of BRs is highly nontrivial since: 1) the coverage region of a BR is characterized by a Cassini oval that presents complex geometry; 2) the coverage regions of different BRs are coupled and the network coverage is intimately related to the locations of all BR nodes. We showed that it is optimal to place BRs on the shortest barrier if it is also the shortest line segment that connects the left and right boundary of the region. Furthermore, we characterized the optimal placement order and spacing of BR nodes on a line segment, both of which present elegant balanced structures.

Although the models are built upon some idealized assumptions, we believe that this work takes an initial step toward understanding the coverage of networked BRs. There are still many questions remaining open. For example, while the Cassini oval sensing model used in this work is based on SNR, it would be interesting to take into account the *Doppler effect*. As the Doppler effect is intimately related to the motion of objects, it would pose a number of challenges in the context of networked radars. In addition, while in this paper we assume that all BRs are homogeneous, a possible future direction is to consider heterogeneous BRs. It is also of interest to take into account the synchronization issue among BR transmitters and BR receivers, which is quite different from that of MRs.

Appendix

Proof of Theorem 1

For any barrier $\widetilde{AB}$ and the optimal placement $\{\mathcal{T}, \mathcal{R}\}$ that minimizes $V(\widetilde{AB})$, we can construct a placement $\{\mathcal{T}', \mathcal{R}'\}$ for $\overline{AB}$ by moving each $T_i \in \mathcal{T}$ and each $R_j \in \mathcal{R}$ to their respective projections $T_i' \in \mathcal{T}'$ and $R_j' \in \mathcal{R}'$ on the line passing through A and B, respectively, as illustrated in Fig. 13. Then, for any point $X' \in \overline{AB}$, there exists a point $X \in \widetilde{AB}$ whose

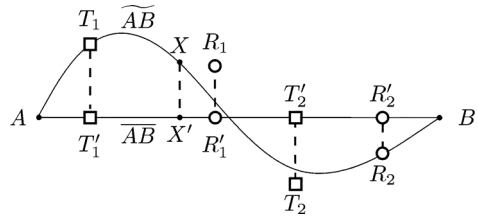

Fig. 13. Snapshot of the proof of Theorem 1.

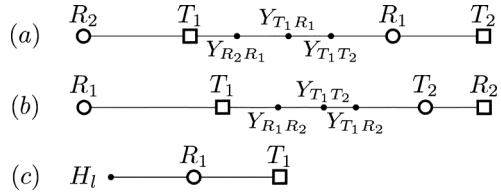

Fig. 14. Snapshots of the proof of Lemma 1: (a) Case 1; (b) Case 2; (c) Case 3.

projection on $\overline{AB}$ is X'. We can observe that $\|T_iX\| \geq \|T_i'X'\|$, $\forall i \in \mathcal{M}$ and $\|R_jX\| \geq \|R_j'X'\|, \forall j \in \mathcal{N}$. Then, it follows that

$$I(X) = \min_{i\in\mathcal{M},j\in\mathcal{N}} \|T_iX\|\|R_jX\| \geq \min_{i\in\mathcal{M},j\in\mathcal{N}} \|T_i'X'\|\|R_j'X'\| = I'(X')$$

where we use $I'(X')$ to denote the detectability of X' under placement $\{\mathcal{T}', \mathcal{R}'\}$. Hence, we have

$$V^*(\overline{AB}) \leq V'(\overline{AB}) = \max_{X'\in\overline{AB}} I'(X') \leq \max_{X\in\widetilde{AB}} I(X) = V^*(\widetilde{AB}) \quad (20)$$

where we use $V'(\overline{AB})$ to denote the vulnerability of $\overline{AB}$ under placement $\{\mathcal{T}', \mathcal{R}'\}$. Since $V^*(U)$ for a line barrier U increases as the length of U increases, and the shortcut barrier H is not longer than $\overline{AB}$, using (20) we have $V^*(H) \leq V^*(\overline{AB}) \leq V^*(\widetilde{AB})$.

Proof of Lemma 1

The main idea of the proof is to divide the line segment between each pair of neighbor nodes into intervals such that all the points on each interval have the *same* closest BR, and then we examine the detectability on each interval. We consider three possible cases of two neighbor nodes as follows.

Case 1: T_1 and R_1 (two nodes of different types).

As illustrated in Fig. 14(a), for any point $X \in \overline{T_1R_1}$, its closest transmitter must be either T_1 or the leftmost transmitter T_2 on $\overline{R_1H_r}$, and its closest receiver must be either R_1 or the rightmost receiver R_2 on $\overline{H_lT_1}$. Suppose the closest BR for a point on $\overline{T_1Y_{R_2R_1}}$, $\overline{Y_{R_2R_1}Y_{T_1T_2}}$, $\overline{Y_{T_1T_2}R_1}$ is T_1-R_2, T_1-R_1, T_2-R_1, respectively. Then, we observe that for $X \in \overline{T_1Y_{R_2R_1}}$, $I(X) = \|R_2X\|\|T_1X\|$ increases as X moves closer to $Y_{R_2R_1}$; for $X \in \overline{Y_{R_2R_1}Y_{T_1T_2}}$, $I(X) = \|T_1X\|\|XR_1\|$ increases as X moves closer to $Y_{T_1R_1}$; for $X \in \overline{Y_{T_1T_2}R_1}$, $I(X) = \|XR_1\|\|XT_2\|$ decreases as X moves closer to R_1. Therefore, $I(X)$ attains maximum on $\overline{T_1R_1}$ when $X = Y_{T_1R_1}$.

Case 2: T_1 and T_2 (two nodes of the same type).

As illustrated in Fig. 14(b), for any point $X \in \overline{T_1T_2}$, its closest transmitter must be either T_1 or T_2, and its closest receiver must be either the rightmost receiver R_1 on $\overline{H_lT_1}$, or the leftmost receiver R_2 on $\overline{T_2H_r}$. Suppose the closest BR for a point on $\overline{T_1Y_{R_1R_2}}$, $\overline{Y_{R_1R_2}Y_{T_1T_2}}$, $\overline{Y_{T_1T_2}T_2}$ is T_1-R_1, T_1-R_2, T_2-R_2, respectively. Then, we observe that for $X \in \overline{T_1Y_{R_1R_2}}$, $I(X) = \|T_1X\|\|R_1X\|$ increases as X moves closer to $Y_{R_1R_2}$; for $X \in \overline{Y_{R_1R_2}Y_{T_1T_2}}$, since X is on the left side of $Y_{T_1R_2}$, $I(X) = \|T_1X\|\|XR_2\|$ increases as X moves closer to $Y_{T_1T_2}$; for $X \in \overline{Y_{T_1T_2}T_2}$, $I(X) = \|XT_2\|\|XR_2\|$ decreases as X moves closer to T_2. Therefore, $I(X)$ attains maximum on $\overline{T_1T_2}$ when $X = Y_{T_1T_2}$.

Case 3: H_l and T_1 (two nodes including an end node).

As illustrated in Fig. 14(c), for any point $X \in \overline{H_lT_1}$, its closest transmitter must be T_1, and its closest receiver must be the leftmost receiver R_1 on $\overline{T_1H_r}$. Hence, the closest BR for a point on $\overline{H_lT_1}$ is T_1-R_1. Then, we observe that for $X \in \overline{H_lT_1}$, $I(X) = \|XT_1\|\|XR_1\|$ increases as X moves closer to H_l, and hence attains maximum when $X = H_l$.

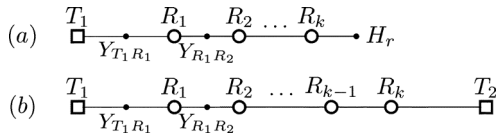

Fig. 15. Snapshots of the proof of Lemma 2: (a) Case 2; (b) Case 3.

Proof of Lemma 2

The main idea of the proof is to sequentially determine the distance between each pair of neighbor nodes. In the following, we consider all three cases of an independent local order $\mathbf{S}_i$ with balanced spacing $\mathbf{D}_{\mathbf{S}_i}$ such that $V(Z_{\mathbf{S}_i}) = c$.

Case 1: $\mathbf{S}_i = (T_1, R_1)$.

Since the closest BR for $Y_{T_1R_1}$ is T_1-R_1, we have $I(Y_{T_1R_1}) = (\|T_1R_1\|/2)^2 = c$. Then, it follows that $\|T_1R_1\| = 2\sqrt{c} = e_c^0$.

Case 2: $\mathbf{S}_i = (T_1, R_1, \ldots, R_k, H_r)$.

Similar to case 1, we can show that $\|T_1R_1\| = 2\sqrt{c} = e_c^0$, as illustrated in Fig. 15(a). Since the closest BR for $Y_{R_1R_2}$ is T_1-R_1 or T_1-R_2, we have

$$I(Y_{R_1R_2}) = \|T_1Y_{R_1R_2}\|\,\|Y_{R_1R_2}R_2\| = \frac{\|T_1R_1\| + \|R_1R_2\|}{2}\frac{\|R_1R_2\|}{2} = c. \quad (21)$$

Then, using (21) and $\|T_1R_1\| = 2\sqrt{c}$, we obtain a unique value $\|R_1R_2\| = e_c^1$. Following this argument recursively, using the values of $\|T_1R_1\|$, $\|R_1R_2\|, \ldots, \|R_{i-1}R_i\|$, we can obtain a unique value $\|R_iR_{i+1}\| = e_c^i$ such that $I(Y_{R_iR_{i+1}}) = c$ for $i = 2, \ldots, k-1$, and at last, using the values of $\|T_1R_1\|$, $\|R_1R_2\|, \ldots, \|R_{k-1}R_k\|$, we can obtain a unique value $\|R_kH_r\| = e_c^k/2$ such that $I(H_r) = c$.

Case 3: $\mathbf{S}_i = (T_1, R_1, \ldots, R_k, T_2)$

Similar to Case 1, we can show that $\|T_1R_1\| = \|R_kT_2\| = e_c^0$, as illustrated in Fig. 15(b). Then, the closest BR for $Y_{R_1R_2}$ must be T_1-R_1 or T_1-R_2. Using the same argument as in Case 2, we can obtain a unique value $\|R_1R_2\| = e_c^1$ such that $I(Y_{R_1R_2}) = c$. Then, the closest BR for $Y_{R_{k-1}R_k}$ must be T_2-R_{k-1} or T_2-R_k. Following the above argument recursively, we can obtain that $\|R_{k-1}R_k\| = e_c^1$, then that $\|R_2R_3\| = e_c^2 \ldots$ until that $\|R_{\frac{k}{2}}R_{\frac{k}{2}+1}\| = e_c^{\frac{k}{2}}$ when k is even, or $\|R_{\frac{k+1}{2}}R_{\frac{k+3}{2}}\| = e_c^{\frac{k-1}{2}}$ when k is odd.

Proof of Lemma 3

The proof is based on contradiction. Suppose there exists another placement $\mathbf{S}_i'$ with spacing $\mathbf{D}_{\mathbf{S}_i'}$ such that $V(Z_{\mathbf{S}_i'}) \leq c$ and

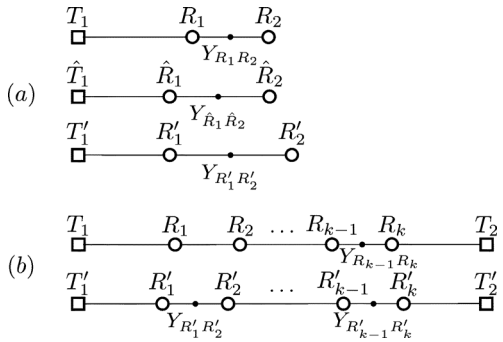

Fig. 16. Snapshots of the proof of Lemma 3: (a) Case 2; (b) Case 3.

$Z_{\mathbf{S}_i} < Z_{\mathbf{S}'_i}$. We consider all three cases of an independent local order $\mathbf{S}_i$ as follows.

Case 1: $\mathbf{S}_i = (T_1, R_1)$.

Since $I(Y_{T'_1R'_1}) = (\|T'_1R'_1\|/2)^2 \le c = I(Y_{T_1R_1}) = (\|T_1R_1\|/2)^2$, we have $\|T'_1R'_1\| \le \|T_1R_1\|$, which is a contradiction.

Case 2: $\mathbf{S}_i = (T_1, R_1, \ldots, R_k, H_r)$.

Similar to Case 1, we can show that $\|T'_1R'_1\| \le \|T_1R_1\|$. Using this and $I'(Y_{R'_1R'_2}) \le c = I(Y_{R_1R_2})$, we next show that $\|T'_1R'_2\| \le \|T_1R_2\|$. Suppose $\|T'_1R'_2\| > \|T_1R_2\|$, as illustrated in Fig. 16(a). Then, we can find a placement $\{\hat{T}_1, \hat{R}_1, \hat{R}_2\}$ such that $\|\hat{T}_1\hat{R}_1\| = \|T'_1R'_1\|$ and $\|\hat{T}_1\hat{R}_2\| = \|T_1R_2\|$. We observe that $\|R'_1R'_2\| > \|\hat{R}_1\hat{R}_2\|$, and hence $\|T'_1Y_{R'_1R'_2}\| > \|\hat{T}_1Y_{\hat{R}_1\hat{R}_2}\|$ and $\|Y_{R'_1R'_2}R'_2\| > \|Y_{\hat{R}_1\hat{R}_2}\hat{R}_2\|$. We also observe that $\|\hat{T}_1\hat{R}_2\|/2 > \|Y_{\hat{R}_1\hat{R}_2}\hat{R}_2\| > \|Y_{R_1R_2}R_2\|$. Using these observations, we have

$$\begin{aligned} I'(Y_{R'_1R'_2}) &= \|T'_1Y_{R'_1R'_2}\|\,\|Y_{R'_1R'_2}R'_2\| \\ &> \|\hat{T}_1Y_{\hat{R}_1\hat{R}_2}\|\|Y_{\hat{R}_1\hat{R}_2}\hat{R}_2\| = \hat{I}(Y_{\hat{R}_1\hat{R}_2}) \\ &> \|T_1Y_{R_1R_2}\|\,\|Y_{R_1R_2}R_2\| = I(Y_{R_1R_2}) \end{aligned} \quad (22)$$

where $\hat{I}(Y_{\hat{R}_1\hat{R}_2})$ denotes the detectability of $Y_{\hat{R}_1\hat{R}_2}$ under placement $\{\hat{T}_1, \hat{R}_1, \hat{R}_2\}$. Then, (22) contradicts that $I'(Y_{R'_1R'_2}) \le I(Y_{R_1R_2})$. Thus, we show that $\|T'_1R'_2\| \le \|T_1R_2\|$.

Following the above argument recursively, using $\|T'_1R'_{i-1}\| \le \|T_1R_{i-1}\|$ and $I(Y_{R_{i-1}R_i}) \ge I'(Y_{R'_{i-1}R'_i})$, we can show that $\|T'_1R'_i\| \le \|T_1R_i\|$ for $i = 2, \ldots, k$, and at last, we can show that $\|T'_1H'_r\| \le \|T_1H_r\|$, which is a contradiction.

Case 3: $\mathbf{S}_i = (T_1, R_1, \ldots, R_k, T_2)$.

Similar to Case 1, we can show that $\|T'_1R'_1\| \le \|T_1R_1\|$ and $\|R'_kT'_2\| \le \|R_kT_2\|$, as illustrated in Fig. 16(b). If the closest transmitter for $Y_{R'_1R'_2}$ is T'_1, similar to case 2, we can show that $\|T'_1R'_2\| \le \|T_1R_2\|$. Next, we show that the closest transmitter for $Y_{R'_1R'_2}$ cannot be T'_2. Suppose the closest transmitter for $Y_{R'_1R'_2}$ is T'_2. Then, we have $\|R'_2T'_2\| \le \|T'_1R'_1\| \le \|T_1R_1\| = \|R_kT_2\|$. Following a similar argument as in Case 2, using $\|R'_2T'_2\| \le \|R_kT_2\|$ and $I'(Y_{R'_1R'_2}) \le I(Y_{R_{k-1}R_k})$, we can show that $\|R'_1T'_2\| \le \|R_{k-1}T_2\|$. Then, it follows that $\|T'_1T'_2\| = \|T'_1R'_1\| + \|R'_1T'_2\| \le \|T_1R_1\| + \|R_{k-1}T_2\| \le \|T_1T_2\|$, which is a contradiction. Thus, we show that the closest transmitter for $Y_{R'_1R'_2}$ cannot be T'_2, and hence must be T'_1.

Using the above argument, we can show that the closest transmitter for $Y_{R'_{k-1}R'_k}$ must be T'_2, and then similar to Case 2, we can show that $\|R'_{k-1}T'_2\| \le \|R_{k-1}T_2\|$. Following this argument recursively, we can show that $\|T'_1R'_3\| \le \|T_1R_3\|$, and then that $\|R'_{k-2}T'_2\| \le \|R_{k-2}T_2\| \ldots$, until we can show that $\|T'_1R'_j\| \le \|T_1R_j\|$ and $\|R'_jT'_2\| \le \|R_jT_2\|$ for $j = \frac{k+1}{2}$ when k is odd or $j = \frac{k}{2} + 1$ when k is even. Then we have $\|T'_1T'_2\| = \|T'_1R'_j\| + \|R'_jT'_2\| \le \|T_1R_j\| + \|R_jT_2\| = \|T_1T_2\|$, which is a contradiction.

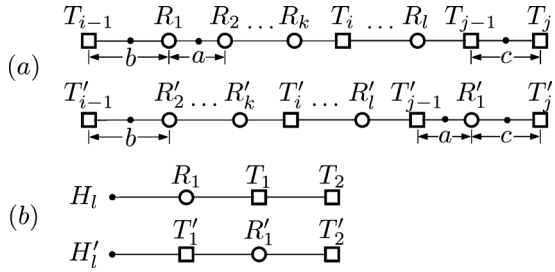

Fig. 17. Snapshots of the proof of Lemma 4: (a) first part; (b) Case 2 of second part.

Proof of Lemma 4

The main idea of this proof is as follows. For any placement $\mathcal{S}$ with an order $\mathbf{S}$ that does not satisfy the condition, we can find another placement $\mathcal{S}'$ with an order $\mathbf{S}'$ that satisfies the condition, such that any local vulnerable value under placement $\mathcal{S}'$, and hence the vulnerability, must be *no greater than* that under placement $\mathcal{S}$. This implies that order $\mathbf{S}'$ is at least as good as order $\mathbf{S}$ (i.e., $f_c^{\mathbf{S}'} \ge f_c^{\mathbf{S}}, \forall c > 0$).

First, we show that there exists an optimal order that satisfies (18a). Consider a placement $\mathcal{S}$ with an order $\mathbf{S}$ that does not satisfy (18a). Then, we can always find some $i \ne j$ such that $n_i \ge 2$, $n_j = 0$, and $n_{j-1} > 0$ or $n_{j+1} > 0$. Without loss of generality, in the following we assume that $n_{j-1} > 0, i \ne 1, M+1$, and $j \ne 1, M+1$, while the other possible cases can be proved using a similar argument. Then, $\mathbf{S}$ includes a local order $(T_{i-1}, R_1, R_2 \ldots, R_k, T_i)$ where $k \ge 2$ and a local order (R_l, T_{j-1}, T_j) [as illustrated in Fig. 17(a)]. We can find another placement $\mathcal{S}'$ with an order $\mathbf{S}'$ constructed from $\mathbf{S}$ by moving R_1 to being between T_{j-1} and T_j. We construct the spacing $\mathbf{D}_{\mathbf{S}'}$ from $\mathbf{D}_{\mathbf{S}}$ by setting $\|T'_{i-1}R'_2\| = \|T_{i-1}R_1\|$, $\|T'_{j-1}R'_1\| = \|R_1R_2\|$, $\|R'_1T'_j\| = \|T_{j-1}T_j\|$, while keeping the distance between each other two neighbor nodes unchanged, such that $\|H_lH_r\| = \|H'_lH'_r\|$. Then, we have $I(Y_{R_1R_2}) \ge I'(Y_{T'_{j-1}R'_1})$, $I(Y_{T_{i-1}R_1}) \ge I'(Y_{T'_{i-1}R'_2})$, and $I(T_{j-1}T_j) \ge I'(R'_1T'_j)$. Furthermore, we can observe that any other local vulnerable value under placement $\mathcal{S}'$ must be no greater than that under placement $\mathcal{S}$. This implies that $\mathbf{S}'$ is at least as good as $\mathbf{S}$. Repeating the above construction, we can always find a order $\mathbf{S}'$ that satisfies (18a), which shows that there must exist an optimal order that satisfies (18a).

Next, we show that among all the orders that satisfy (18a), there exists an optimal order that also satisfies (18b), and it is dividable. We consider two cases of an order $\mathbf{S}$ that satisfies (18a) as follows.

Case 1: $M < N$.

Since $\mathbf{S}$ satisfies (18a), we must have $n_i > 0$ for each $i = 1, \ldots, M+1$, and hence (18b) is also satisfied. Then, $\mathbf{S}$ can be decomposed into independent local orders as

$$\mathbf{S} = (\overbrace{H_l, \ldots, \underbrace{T_1}_{\mathbf{S}_2}, \ldots, T_2}^{\mathbf{S}_1}, \ldots, \overbrace{T_{M-1}, \ldots, \underbrace{T_M}_{\mathbf{S}_{M+1}}, \ldots, H_r}^{\mathbf{S}_M}) \quad (23)$$

and hence is dividable.

Case 2: $M = N$.

Suppose order $\mathbf{S}$ does not satisfy (18b). Then, we must have $n_2 = 0$ and $n_i = 1, \forall i \neq 2$, or $n_M = 0$ and $n_i = 1, \forall i \neq M$. Suppose the former case holds without loss of generality. Then, for any placement $\mathcal{S}$ with order $\mathbf{S}$, we can find another placement $\mathcal{S}'$ constructed from $\mathcal{S}$ by swapping the locations of node R_1 and node T_1, such that $\mathcal{S}'$ has an order $\mathbf{S}'$ that satisfies (18b) [as illustrated in Fig. 17(b)]. Then, we observe that any local vulnerable value under placement $\mathcal{S}'$ must be no greater than that under placement $\mathcal{S}$, which implies that order $\mathbf{S}'$ is at least as good as order $\mathbf{S}$. Thus, there must exist an optimal order that satisfies both (18a) and (18b).

For an order $\mathbf{S}$ that satisfies (18), we consider two cases: 1) if $n_1 = 0$ and $n_i = 1, \forall i \neq 1$, then $\mathbf{S}$ can be decomposed into independent local orders as

$$\mathbf{S} = (\overbrace{H_{\rm l}, T_1, \underbrace{R_1}_{\mathbf{S}_2}}^{\mathbf{S}_1}, \overbrace{\underbrace{T_2}_{\mathbf{S}_3}, R_2, T_3}^{\mathbf{S}_3}, \ldots, \overbrace{T_{M-1}, R_{M-1}, \underbrace{T_M}_{\mathbf{S}_M}, R_M, H_{\rm r}}^{\mathbf{S}_{M+1}}) \quad (24)$$

and hence is dividable. Similarly, $\mathbf{S}$ is also dividable if $n_{M+1} = 0$ and $n_i = 1, \forall i \neq M+1$; 2) if $n_k = 0$ where $k \neq 1, 2, M, M+1$ and $n_i = 1, \forall i \neq k$, then $\mathbf{S}$ can be decomposed into independent local orders as in (25), and hence is dividable

$$\begin{aligned}\mathbf{S} = (&\overbrace{H_{\rm l}, R_1, \underbrace{T_1}_{\mathbf{S}_2}, R_2, T_2}^{\mathbf{S}_1}, \ldots, \\ &\overbrace{T_{k-2}, \underbrace{R_{k-1}}_{\mathbf{S}_k}, T_{k-1}, T_k, \underbrace{R_k}_{\mathbf{S}_k}, T_{k+1}}^{\mathbf{S}_{k-1}, \mathbf{S}_{k+1}}, \ldots, \\ &\overbrace{T_{M-1}, R_{M-1}, \underbrace{T_M}_{\mathbf{S}_M}, R_M, H_{\rm r}}^{\mathbf{S}_{M+1}}). \end{aligned} \quad (25)$$

Proof of Theorem 3

By Lemma 4, there exists an optimal order among all the orders that satisfy (18), which are dividable. We observe that any order that satisfies (19) also satisfies (18). Therefore, it suffices to show that for any two orders $\mathbf{S}$ and $\mathbf{S}'$ that satisfy (18): 1) if $\mathbf{S}$ satisfies (19) and $\mathbf{S}'$ does not satisfy (19), then $f_c^{\mathbf{S}} \geq f_c^{\mathbf{S}'}$; 2) if $\mathbf{S}$ and $\mathbf{S}'$ both satisfy (19), then $f_c^{\mathbf{S}} = f_c^{\mathbf{S}'}$.

Let $g_c(n)$ denote the optimal value of problem (16) for an independent local order $\mathbf{S}_i$ with type (T, R^n, T) or (R, T^n, R) under the constraint $V(Z_{\mathbf{S}_i}) \leq c$. By Lemmas 2 and 3, we have

$$g_c(n) = \begin{cases} 2\sum_{i=0}^{\frac{n}{2}-1} e_c^i + e_c^{\frac{n}{2}}, & \text{if } n \text{ is even} \\ 2\sum_{i=0}^{\frac{n+1}{2}-1} e_c^i, & \text{if } n \text{ is odd.} \end{cases} \quad (26)$$

Then, it follows from (26) that

$$g_c(n+1) - g_c(n) = \begin{cases} e_c^{\frac{n}{2}}, & \text{if } n \text{ is even} \\ e_c^{\frac{n+1}{2}}, & \text{if } n \text{ is odd.} \end{cases} \quad (27)$$

Next, we consider two cases of an order $\mathbf{S}$ that satisfies (18).

Case 1: $M < N$.

We have shown in the proof of Lemma 4 that $\mathbf{S}$ can be decomposed into independent local orders as (23). Using Theorem 2 and (23), we have

$$f_c^{\mathbf{S}} = \sum_{i=2}^{M} g_c(n_i) + \frac{g_c(2n_1)}{2} + \frac{g_c(2n_{M+1})}{2}. \quad (28)$$

Without loss of generality, suppose $\mathbf{S}$ does not satisfy (19). The case where $\mathbf{S}$ does not satisfy (19b) can be proved using a similar argument. Then, there exist $i, j \in \{2, \ldots, M\}$ such that $n_i \geq n_j + 2$. We can find another order $\mathbf{S}'$ with $\mathbf{N}_{\mathbf{S}'} = \{n_1', \ldots, n_{M+1}'\}$ constructed from $\mathbf{N}_{\mathbf{S}}$ by setting $n_i' = n_i - 1$, $n_j' = n_j + 1$, and $n_k' = n_k, \forall k \neq i, j$. Using (28) and (27), we have

$$\begin{aligned} f_c^{\mathbf{S}} - f_c^{\mathbf{S}'} &= g_c(n_i) - g_c(n_i - 1) + g_c(n_j) - g_c(n_j + 1) \\ &= \begin{cases} e_c^{\frac{n_i}{2}}, & \text{if } n_i \text{ is even} \\ e_c^{\frac{n_i-1}{2}}, & \text{if } n_i \text{ is odd} \end{cases} \\ &\quad - \begin{cases} e_c^{\frac{n_j}{2}}, & \text{if } n_j \text{ is even} \\ e_c^{\frac{n_j+1}{2}}, & \text{if } n_j \text{ is odd} \end{cases} \\ &\leq 0 \end{aligned}$$

which shows that $\mathbf{S}$ is not optimal. Furthermore, for any two orders $\mathbf{S}$ and $\mathbf{S}'$ that both satisfy (19), we can show that $f_c^{\mathbf{S}} = f_c^{\mathbf{S}'}$. Therefore, any order that satisfies (19) is optimal.

Case 2: $M = N$.

Suppose $\mathbf{S}$ does not satisfy (19). Then, we have $n_k = 0$ where $k \neq 1, 2, M, M+1$ and $n_i = 1, \forall i \neq k$. Using (25), we have

$$f_c^{\mathbf{S}} = (M-4)g_c(1) + 2g_c(2) + 2e_c^0. \quad (29)$$

Suppose another order $\mathbf{S}'$ satisfies (19) with $\mathbf{N}_{\mathbf{S}'} = \{n_1', \ldots, n_{M+1}'\}$ such that $n_1' = 0$ and $n_i' = 1, \forall i \neq 1$. Using (24), we have

$$f_c^{\mathbf{S}'} = (M-2)g_c(1) + g_c(2) + e_c^0. \quad (30)$$

It follows from (29) and (30) that

$$f_c^{\mathbf{S}} - f_c^{\mathbf{S}'} = g_c(2) + e_c^0 - 2g_c(1) = e_c^1 - e_c^0 < 0 \quad (31)$$

which shows that $\mathbf{S}$ is not optimal. Furthermore, for any two orders $\mathbf{S}$ and $\mathbf{S}'$ that both satisfy (19), we can show that $f_c^{\mathbf{S}} = f_c^{\mathbf{S}'}$. Therefore, any order that satisfies (19) is optimal.

REFERENCES

[1] X. Gong, J. Zhang, and D. Cochran, "Barrier coverage in bistatic radar sensor networks: Cassini oval sensing and optimal placement," in *Proc. ACM MobiHoc*, 2013, pp. 49–58.

[2] C. J. Baker and H. D. Griffiths, "Bistatic and multistatic radar sensors for homeland security," *Adv. Sensing Security Appl.*, vol. 2, pp. 1–22, Feb. 2006.

[3] B. Donovan, D. J. McLaughlin, and J. Kurose, "Principles and design considerations for short-range energy balanced radar networks," in *Proc. IEEE IGARSS*, 2005, pp. 2058–2061.

[4] S. Kumar, T.-H. Lai, and A. Arora, "Barrier coverage with wireless sensors," in *Proc. ACM MobiCom*, 2005, pp. 284–298.

[5] A. Chen, T.-H. Lai, and D. Xuan, "Measuring and guaranteeing quality of barrier-coverage in wireless sensor networks," in *Proc. ACM MobiHoc*, 2008, pp. 421–430.

[6] B. Liu, O. Dousse, J. Wang, and A. Saipulla, "Strong barrier coverage of wireless sensor networks," in *Proc. ACM MobiHoc*, 2008, pp. 411–420.

[7] A. Saipulla, B. Liu, G. Xing, X. Fu, and J. Wang, "Barrier coverage with sensors of limited mobility," in *Proc. ACM MobiHoc*, 2010, pp. 201–210.

[8] B. Wang, "Coverage problems in sensor networks: A survey," *Comput. Surveys*, vol. 43, no. 4, Oct. 2011, Art. no. 32.

[9] N. Willis, *Bistatic Radar*. Raleigh, NC, USA: SciTech, 2005.

[10] J. Liang and Q. Liang, "Orthogonal waveform design and performance analysis in radar sensor networks," in *Proc. IEEE MILCOM*, 2006, pp. 1–6.
[11] H.-D. Ly and Q. Liang, "Collaborative multi-target detection in radar sensor networks," in *Proc. IEEE MILCOM*, 2007, pp. 1–7.
[12] J. Liang and Q. Liang, "Design and analysis of distributed radar sensor networks," *IEEE Trans. Parallel Distrib. Syst.*, vol. 27, no. 11, pp. 1926–1933, Nov. 2011.
[13] H. Deng, "Orthogonal netted radar systems," *IEEE Aerosp. Electron. Syst. Mag.*, vol. 27, no. 5, pp. 28–35, May 2012.
[14] E. Paolini, A. Giorgetti, M. Chiani, R. Minutolo, and M. Montanari, "Localization capability of cooperative anti-intruder radar systems," *EURASIP J. Adv. Signal Process.*, vol. 2008, p. 726854, 2008.
[15] S. Meguerdichian, F. Koushanfar, M. Potkonjak, and M. Srivastava, "Coverage problems in wireless ad-hoc sensor networks," in *Proc. IEEE INFOCOM*, 2001, vol. 3, pp. 1380–1387.
[16] S. Meguerdichian, S. Slijepcevic, V. Karayan, and M. Potkonjak, "Localized algorithms in wireless ad-hoc networks: Location discovery and sensor exposure," in *Proc. ACM MobiHoc*, 2001, pp. 106–116.
[17] X.-Y. Li, P.-J. Wan, and O. Frieder, "Coverage in wireless ad hoc sensor networks," *IEEE Trans. Comput.*, vol. 52, no. 6, pp. 753–763, Jun. 2003.
[18] M. Skolnik, *Introduction to Radar Systems*. New York, NY, USA: McGraw-Hill, 2002.
[19] A. A., P. Dutta, and S. Bibyk, "Towards radar-enabled sensor networks," in *Proc. ACM/IEEE IPSN*, 2006, pp. 467–474.
[20] Q. Liang, "Waveform design and diversity in radar sensor networks: Theoretical analysis and application to automatic target recognition," in *Proc. IEEE SECON*, 2006, vol. 2, pp. 684–689.
[21] T. Hanselmann, M. Morelande, B. Moran, and P. Sarunic, "Constrained multi-object Markov decision scheduling with application to radar resource management," in *Proc. Inf. Fusion*, 2010, pp. 1–8.
[22] M. Li *et al.*, "Multi-user data sharing in radar sensor networks," in *Proc. ACM SenSys*, 2004, pp. 247–260.
[23] S. Bartoletti, S. Conti, and A. Giorgetti, "Analysis of UWB radar sensor networks," in *Proc. IEEE ICC*, 2010, pp. 1–6.
[24] X. Gong, J. Zhang, and D. Cochran, "When target motion matters: Doppler coverage in radar sensor networks," in *Proc. IEEE INFOCOM*, 2013, pp. 1169–1177.
[25] S. Meguerdichian, F. Koushanfar, G. Qu, and M. Potkonjak, "Exposure in wireless ad-hoc sensor networks," in *Proc. ACM MobiCom*, 2001, pp. 139–150.
[26] R.-H. Gau and Y.-Y. Peng, "A dual approach for the worst-case-coverage deployment problem in ad-hoc wireless sensor networks," in *Proc. IEEE MASS*, 2006, pp. 427–436.
[27] C. Lee, D. Shin, S.-W. Bae, and S. Choi, "Best and worst-case coverage problems for arbitrary paths in wireless sensor networks," in *Proc. IEEE MASS*, 2010, pp. 127–136.
[28] G.-Y. Keung, B. Li, and Q. Zhang, "The intrusion detection in mobile sensor network," in *Proc. ACM MobiHoc*, 2010, pp. 11–20.
[29] Y. Wang and G. Cao, "Barrier coverage in camera sensor networks," in *Proc. ACM MobiHoc*, 2011, Art. no. 12.
[30] H. Ma, Y. Meng, D. Li, Y. Hong, and W. Chen, "Minimum camera barrier coverage in wireless camera sensor networks," in *Proc. IEEE INFOCOM*, 2012, pp. 217–225.

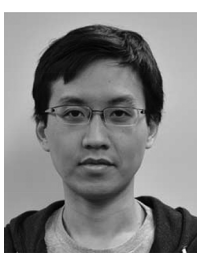

Xiaowen Gong (S'12) received the B.Eng. degree in electronics and information engineering from Huazhong University of Science and Technology, Wuhan, China, in 2008, and the M.Sc. degree in electrical engineering from the University of Alberta, Edmonton, AB, Canada, in 2010, and is currently pursuing the Ph.D. degree in electrical engineering at Arizona State University, Tempe, AZ, USA.

His research interests include mobile social networks, sensor networks, cognitive radio networks, and relay networks.

Junshan Zhang (S'98–M'00–SM'06–F'12) received the Ph.D. degree in electrical and computer engineering from Purdue University, West Lafayette, IN, USA, in 2000.

He joined the School of Electrical, Computer and Energy Engineering (ECEE), Arizona State University, Tempe, AZ, USA, in 2000, where he has been a Professor since 2010. His interests include cyber-physical systems, communications networks, and network science. His current research focuses on fundamental problems in information networks and energy networks, including modeling and optimization for smart grid, network optimization/control, mobile social networks, crowdsourcing, cognitive radio, and network information theory.

Prof. Zhang was an Associate Editor for the IEEE TRANSACTIONS ON WIRELESS COMMUNICATIONS, an Editor for *Computer Networks*, and an Editor for the *IEEE Wireless Communication Magazine*. He is currently serving as an Editor-at-Large for the IEEE/ACM TRANSACTIONS ON NETWORKING and an Editor for the *IEEE Network*. He is a Distinguished Lecturer of the IEEE Communications Society. He was TPC Co-Chair for a number of major conferences in communication networks, including INFOCOM 2012, WICON 2008, and IPCCC 2006, and TPC Vice Chair for ICCCN 2006. He was the General Chair for the IEEE Communication Theory Workshop 2007. He is a recipient of the ONR Young Investigator Award in 2005 and the NSF CAREER Award in 2003. He received the Outstanding Research Award from the IEEE Phoenix Section in 2003. He coauthored a paper that won the IEEE ICC 2008 Best Paper Award and two papers that won the Best Paper Runner-up Award of IEEE INFOCOM 2009 and IEEE INFOCOM 2014.

Douglas Cochran (S'86–A'90–M'92–SM'96) received the B.S. degree in mathematics from the Massachusetts Institute of Technology (MIT), Cambridge, MA, USA, in 1987, the M.S. degree in mathematics from the University of California, San Diego, La Jolla, CA, USA, in 1980, and the S.M. and Ph.D. degrees in applied mathematics from Harvard University, Cambridge, MA, USA, in 1986 and 1990, respectively.

Since 1989, he has been on the faculty of the School of Electrical, Computer and Energy Engineering, Arizona State University (ASU), Tempe, AZ, USA, and is also affiliated with the School of Mathematical and Statistical Sciences. Between 2005 and 2008, he served as Assistant Dean for Research with the Ira A. Fulton School of Engineering, ASU. Between 2000 and 2005, he was Program Manager for Mathematics with the Defense Advanced Research Projects Agency (DARPA), and he held a similar position with the US Air Force Office of Scientific Research between 2008 and 2010. Prior to joining the ASU faculty, he was a Senior Scientist with BBN Systems and Technologies, Inc., Cambridge, MA, USA, during which time he served as Resident Scientist with the DARPA Acoustic Research Center and the Naval Ocean Systems Center. He has been a Visiting Scientist with the Australian Defense Science and Technology Organization and served as a consultant to several technology companies. His research is in applied harmonic analysis and statistical signal processing.

Prof. Cochran is Technical Program Co-Chair for the 2015 IEEE International Conference on Acoustics, Speech, and Signal Processing (ICASSP 2015), and he was General Co-Chair of the ICASSP 1999 and Co-Chair of the 1997 U.S.-Australia Workshop on Defense Signal Processing. He has also served as Associate Editor for book series and journals, including the IEEE TRANSACTIONS ON SIGNAL PROCESSING.

Dr. Kai Xing (S'07–A'08–M'13) received the M.S. and Ph.D. degrees in computer science from The George Washington University, Washington, DC, USA, in 2006 and 2009, respectively.

He is an Associate Professor with the Department of Computer Science and Technology, The University of Science and Technology of China, Hefei, China. His current research interests include cyber-physical networking systems, mobile computing, in-network information processing, and network security.

Dr. Xing is a member of the Association for Computing Machinery (ACM).